Journal of Organometallic Chemistry 695 (2010) 2076–2082

Contents lists available at ScienceDirect

Journal of Organometallic Chemistry

journal homepage: www.elsevier.com/locate/jorganchem

{(COD)Ru[RN=C(H)–C(H)=C(Ph)]$_2$} (R=Me, Et): The first structurally characterized mononuclear ruthenium complexes with enyl-imino ligands and their relevance in ruthenium catalyzed C–H activation reactions

Linda Schweda, Andreas Nader, Roberto Menzel, Tobias Biletzki, Christopher Johne, Helmar Görls, Wolfgang Imhof*

Institute of Inorganic and Analytical Chemistry, Friedrich-Schiller-University Jena, August-Bebel-Str. 2, 07743 Jena, Germany

A R T I C L E   I N F O

Article history:
Received 9 February 2010
Received in revised form
3 May 2010
Accepted 16 May 2010
Available online 24 May 2010

Dedicated to Prof. Dr. Uwe Rosenthal on the occasion of his 60th birthday.

Keywords:
Ruthenium
Imines
C–H activation
Catalysis
Lactams
X-ray

A B S T R A C T

The reaction of α,β-unsaturated imines with [(1,5-cyclooctadiene)-bis(2-methylallyl)-ruthenium(II)] leads to the formation of mononuclear ruthenium complexes of the general formula {(COD)Ru[RN=C(H)–C(H)=C(Ph)]$_2$}. In these complexes the imine ligands are deprotonated in β-position with respect to the imine double bond and coordinate as an enyl-imino ligand. In the case of R = Me, Et the corresponding compounds have been characterized by X-ray crystallography. The relevance of these complexes with respect to ruthenium catalyzed C–C coupling reactions of the same α,β-unsaturated imines is demonstrated by the structural analysis of another mononuclear ruthenium complex in which two imine ligands are reductively coupled (R = Cy). [(1,5-Cyclooctadiene)-bis(2-methylallyl)-ruthenium(II)] also turns out to be a highly effective precatalyst in the reaction of the respective imines with carbon monoxide and ethylene to produce heterocyclic compounds.

© 2010 Elsevier B.V. All rights reserved.

1. Introduction

Monoazadiene ruthenium chemistry has been extensively carried out in the last decades of the 20th century and has been summarized in a review article by Elsevier et al. [1]. This research was mainly triggered by the anticipated analogy of monoazadiene chemistry with the well-known coordination chemistry of 1,3-butadienes and 1,4-diazadienes. Treatment of monoazadienes with $Ru_3(CO)_{12}$ results in the formation of a wide variety of mono-, di, tri- and tetra-nuclear ruthenium carbonyl complexes depending on stoichiometry, reaction temperature and reaction time. All structurally characterized ruthenium monoazadiene complexes up to now therefore are ruthenium carbonyl species. In most of these compounds the monoazadiene is deprotonated in β-position with respect to the imine double bond. Coordination of the imine nitrogen and the respective β-carbon atom leads to a planar five-membered aza-ruthena-cyclopentadienyl system that is bonded to another transition metal in a η^3- or η^5-fashion [2]. Only one structurally characterized compound in which the monoazadiene coordinates as a neutral ligand has been described [3]. In this complex ruthenium is bonded in a η^4-fashion to the C=C and C=N double bonds and is therefore observed below the essentially planar ligand system. The latter coordination mode is commonly observed in the case of the corresponding iron tricarbonyl complexes.

In the presence of catalytic amounts of ruthenium complexes (mostly $Ru_3(CO)_{12}$ is used) α,β-unsaturated imines may be reacted with suitable additional substrates as alkenes, alkynes, isocyanides or carbon monoxide to produce a wide variety of organic products [4]. These reactions proceed *via* a C–H activation in the same position as it is observed in the formation of monoazadiene ruthenium complexes in stoichiometric reactions.

In this paper we describe the synthesis and structural characterization of monoazadiene complexes derived from [(1,5-cyclooctadiene)-bis(2-methylallyl)-ruthenium(II)] as well as the use of this ruthenium complex as an effective precatalyst in catalytic C–H activation reactions.

* Corresponding author. Tel.: +49 3641 948 185; fax: +49 3641 948 102.
E-mail address: Wolfgang.Imhof@uni-jena.de (W. Imhof).

0022-328X/$ – see front matter © 2010 Elsevier B.V. All rights reserved.
doi:10.1016/j.jorganchem.2010.05.020

2. Results and discussion

The reaction of [(1,5-cyclooctadiene)-bis(2-methylallyl)-ruthenium(II)], **1**, with imines **2a**–**c** that are derived from cinnamaldehyde and the respective aliphatic primary amines yields mononuclear ruthenium complexes **3a**, **3b** or **4** depending on the nitrogen bound aliphatic group (Scheme 1). In all complexes one (**4**) or two (**3a**, **3b**) deprotonated imine ligands are observed coordinating to ruthenium as an enyl-imino ligand. In compounds of type **3** coordination environment of ruthenium is completed by 1,5-cyclooctadiene. In complex **4** ruthenium is coordinated by an additional ligand that is obviously formed by the reductive coupling of two imines.

The driving force of these reactions most probably is the elimination of isobutene that is formed from the allyl ligands in **1** and the hydrogen atoms that are produced from C–H activation reactions of imine ligands. Headspace GC-MS spectra show the presence of isobutene next to 1,5-, 1,4- and 1,3-cyclooctadiene, the latter most probably being produced by ruthenium catalyzed alkene isomerization from 1,5-cyclooctadiene ligands (*cf.* Supplementary material). Moreover, in all MS spectra of crude reaction mixtures compounds of the general formula {(1,5-cyclooctadiene)-(2-methylallyl)-[RN=C(H)–C(H)=C(Ph)]–ruthenium(II)} are observed next to compounds of type **3** and **4**. Nevertheless, these mixtures were not separable by column chromatography due to extensive decomposition. The main products of the reactions of **2a**–**c** were therefore obtained by fractionate crystallization yielding crystals of **3a**, **3b** and **4** that were suitable for X-ray diffraction. We are therefore convinced that the reactions proceed *via* subsequent addition and C–H activation of the imine ligands and not *via* the elimination of a dimerization product of the allyl ligands, e.g. 2,5-dimethyl-1,5-hexadiene, which is not detectable by any analytical method we applied.

The molecular structures of **3a** and **3b** are presented in Figs. 1 and 2, respectively. The most important bond lengths and angles are depicted in Table 1. **3a** and **3b** are the first structurally characterized mononuclear ruthenium complexes with unsaturated imine ligands being coordinated in an enyl-imino fashion. In addition, to the best of our knowledge they are also the first CO free ruthenium complexes of this kind at all. A highly related complex of the formula {[^{i}PrN=C(H)–C(H)=C(R)]Ru(CO)$_2$(PPh$_3$)Cl} has been synthesized from the chloride bridged dimeric compound {[^{i}PrN=C(H)–C(H)=C(R)]$_2$Ru$_2$(CO)$_4$(μ_2 – Cl)$_2$} by cleaving the halogen bridges with Lewis basic triphenylphosphine [3]. Nevertheless, there is no structural information on this compound. **3a** and **3b** both show the central ruthenium atom in a distorted octahedral coordination geometry. The two nitrogen atoms are in *trans*-position with respect to each other and ruthenium nitrogen bond lengths are measured to 213.1(1) and 213.4(2) pm for **3a** and 215.0 (2) and 215.4(2) pm for **3b**. The bonds between ruthenium and the formally negatively charged carbon atoms are 205.1(2) and 205.0 (2) pm for **3a** and 205.5(2) and 205.2(2) pm for **3b**. Phenyl substituents are twisted out of the plane defined by the enyl-imino ligand (torsion angles for **3a**: 103.7(9)° and 116.7(9)°, **3b**: 106.7(9)° and 110.8(9)°). As it is expected 1,5-cyclooctadiene coordinates *via* both carbon carbon double bonds.

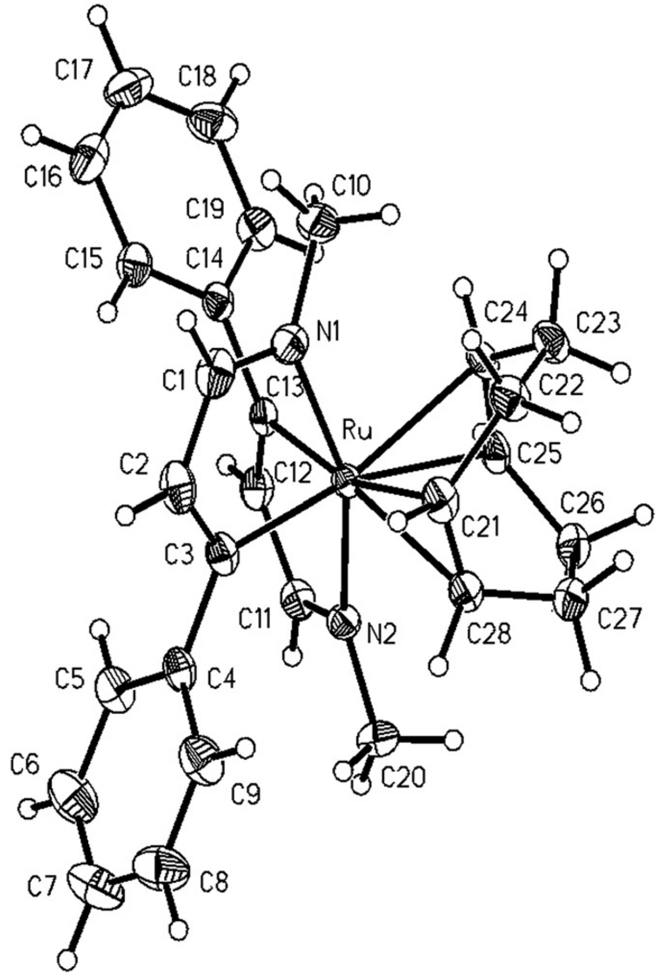

Fig. 1. Molecular structure of **3a**. Thermal ellipsoids are depicted on the 40% probability level.

Fig. 1 shows the Δ-isomer of **3a** whereas in Fig. 2 the Λ-isomer of **3b** is depicted. Nevertheless, due to the presence of crystallographic centers of inversion (space groups **3a**: $P\overline{1}$, **3b**: $P2_1/c$) both enantiomers are present in the crystal structure. In principle another pair of enantiomeric stereoisomers might be formed in which the nitrogen atoms are arranged in *cis*-position. We therefore calculated the Δ- and Λ-enantiomers of both *cis*- and *trans*-configurated stereosiomers of **3b** using DFT methods with the unrestricted B3LYP functional and a 6–31* basis set [5]. Relativistic effects of ruthenium have been taken into account by applying Stuttgart-Dresden pseudo potentials as implemented in GAUSSIAN03. No symmetry constraints whatsoever have been considered. All

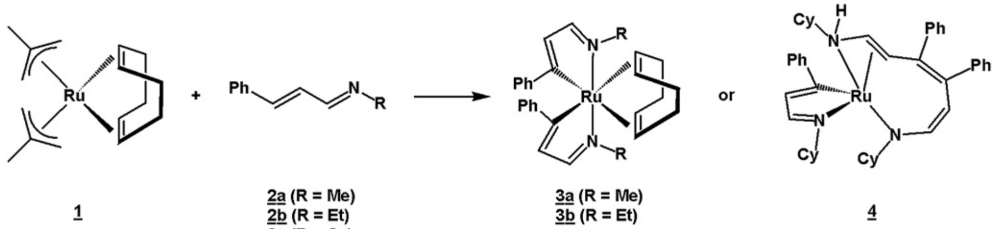

Scheme 1. Synthesis of mononuclear ruthenium enyl-imino complexes **3a**, **b** and **4**.

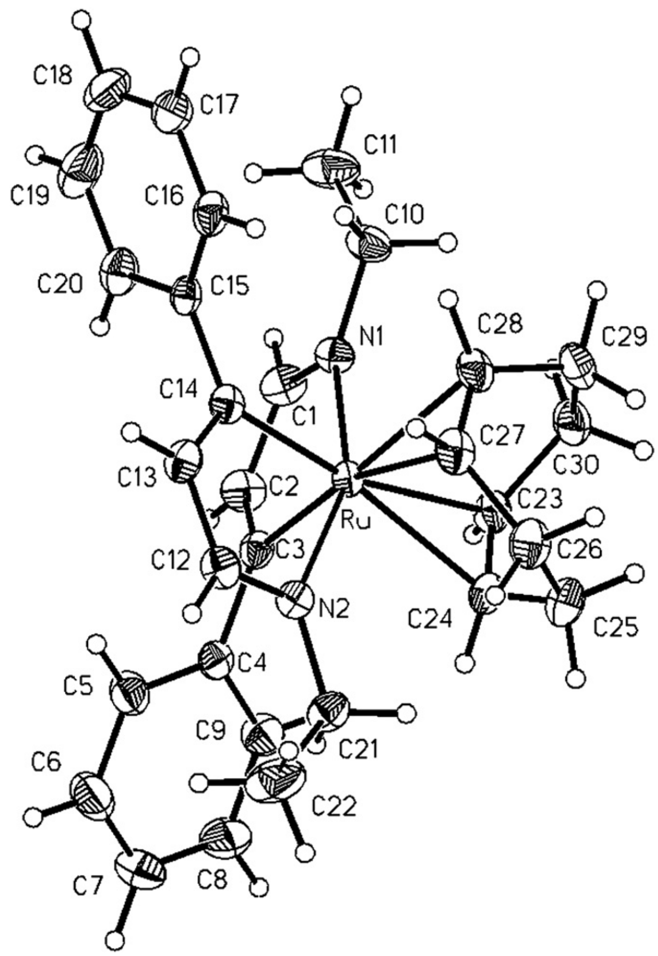

Fig. 2. Molecular structure of **3b**. Thermal ellipsoids are depicted on the 40% probability level.

structures were fully optimized and additional frequency calculations were performed. There are no imaginary frequencies in the calculations of all theoretically investigated compounds meaning that the reported structures are truly minimum structures on the energy hyper surface. Molecular structures of four calculated stereoisomers of **3b** are shown in Fig. 3. Of course, enantiomeric structures exhibit identical bond lengths and angles which in the case of the *trans*-isomers nicely correspond to the experimentally observed values (Table 2). Due to different *trans*-effects Ru–N and Ru–C bonds in *cis*-**3b** show two distinctively different values in the calculated structure of *cis*-**3b** and they also significantly differ from those observed for *trans*-**3b**. Enantiomers as expected also show the same energy. Nevertheless, we observed the *trans*-isomers to be 17.6 kJ mol^{-1} more stable then the corresponding *cis*-isomers. The formation of **3a** and **3b** therefore is most probably a thermodynamically controlled process.

NMR spectroscopic investigations also confirm the presence of only one set of signals corresponding to the isomers of **3a** and **3b** with the nitrogen atoms being situated in a *trans*-configuration. Chemical shifts of the enyl-imino ligands in ^{1}H as well as ^{13}C spectra are very similar to the data presented for the highly related complex {[^{i}PrN=C(H)–C(H)=C(R)]Ru$(CO)_2$$(PPh_3)$Cl} [3]. Most significantly ^{13}C resonances representing the formally negatively charged C_β are significantly shifted downfield (**3a**: 231.6 ppm, **3b**: 236.3 ppm). For **3a** hydrogen atoms at C_α and C_β give rise to isolated doublets at 6.26 and 7.79 ppm with a coupling constant of 4.0 Hz. Corresponding protons in **3b** show a doublet at 8.07 ppm with a coupling constant of 6.0 Hz for the proton at C_α whereas the signal for $C_\beta H$ overlaps with signals of aromatic protons. Resonances of phenyl, methyl (**3a**) and ethyl (**3b**) substitutents as for coordinated COD are observed in expected regions of the spectra.

If imine **2c** with a nitrogen bonded cyclohexyl group is reacted with ruthenium complex **1** another mononuclear coordination compound is obtained by fractionate crystallization from the crude reaction mixture. Complex **4** formally displays a molecular composition [RuL(L–H)$_2$]. MS spectra of the crude reaction mixtures of the reactions of **2a** and **2b** also show the presence of compounds with this molecular composition. Besides, we were not able to isolate them in addition to the above described compounds **3a** and **3b**.

The molecular structure of **4** is depicted in Fig. 4, most important bond lengths and angles are also summarized in Table 1. In contrast to **3a** and **3b** cyclooctadiene is not observed as a ligand in **4** any more. The complete coordination sphere of Ru in **4** is constructed from ligands derived from the imine starting compound **2c**. The compound is best described as a Ru(II) complex with two anionic ligands. Ruthenium is observed in a slightly distorted square-pyramidal coordination sphere with the nitrogen atoms and the centroid of C1 and C2 (X1A) forming the basis of the polyhedron. Mean deviations from the ideal plane are 5.9 (N1), 4.0 (N2), 3.7 (N3) and 6.2 (X1A) pm. Ruthenium is observed slightly above this plane (13.4 pm) and the formally anionic carbon atom C33 represents the apex of the pyramid.

One ligand (N3, C31–C45) is an enyl-imino ligand identical to the ones described for **3a** and **3b** that is produced by deprotonation of the imine **1c** in β-position with respect to the imine double bond and acting as a chelating ligand. Bond lengths and angles of this ligand are also well comparable to the situation in **3a** and **3b** although the corresponding Ru–N3 bond is significantly shorter as in the latter compounds. This may be due to the different electronic properties of the coordinating olefinic double bond in *trans*-position compared to the second imine nitrogen being in *trans*-position in **3a** and **3b**. Calculations of the *cis*-isomers of **3b** have also demonstrated the significant effect of a change of *trans*-ligands on Ru–N bond lengths (Table 2). The second ligand obviously has been formed by a metal induced dimerization of two ligands **2c** (N1, C1–C15 and N2, C16–C30). Coupling of the ligands occurred by establishing a new carbon carbon bond between the two carbon atoms in β-position to each imine bond. As a result one of the former imine nitrogen atoms (N_2) now coordinates as a formally negatively charged imido nitrogen showing the by far shortest Ru–N bond length. The chain of six carbon atoms (C16–C17–C18–C3–C2–C1) is an extended conjugated system with the bond lengths therefore being quite similar. The C1–C2 double bond shows a side-on coordination to the central ruthenium. Coordination of ruthenium is completed by N1 which is protonated in **4** leading to the formulation of the N1–C1–C2 moiety to represent a η^3-enamine system. The position of the respective hydrogen has been determined from the difference Fourier map and it has been freely refined. A transfer of a hydrogen atom from a carbon atom in β-position with respect to an imine double bond toward the former imine nitrogen atom has been described by some of us before in the reaction of β-naphthylimines with $Fe_2(CO)_9$ [6].

NMR spectra of **4** nicely reflect the molecular structure. Nevertheless, due to the significant changes in the environment of ruthenium ^{13}C resonances of the enyl-imino ligand (C31–C33 in Fig. 4) are observed at different chemical shifts compared to complexes of type **3**. The quaternary carbon atom shows a chemical shift of 193.8 ppm and is therefore shifted upfield compared to **3a** and **3b** whereas the other two carbon atoms of this ligand backbone are only slightly shifted. Olefinic carbon atoms are observed from the aromatic region of the spectrum up to approximately 82 ppm. It is also obvious that there are more signals representing cyclohexyl substituents than are expected. This may be explained by the assumption that two of the cyclohexyl moieties are not able to

Table 1
Selected bond lengths [pm] and angles [°] of **3a**, **3b** and **4**.

3a							
Ru–N1	213.4(2)	Ru–C3	205.1(2)	Ru–N2	213.1(1)	Ru–C13	205.0(2)
Ru–C21	228.6(2)	Ru–C24	228.8(2)	Ru–C25	228.4(2)	Ru–C28	230.2(2)
N1–C1	129.5(3)	C1–C2	142.1(3)	C2–C3	136.2(3)	N2–C11	129.2(2)
C11–C12	141.9(3)	C12–C13	136.9(2)				
N1–Ru–N2	158.76(6)	N1–Ru–C3	77.37(7)	N1–Ru–C13	88.76(6)	N2–Ru–C3	87.98(6)
N2–Ru–C13	77.52(6)	C3–Ru–C13	96.30(7)	N1–Ru–X1A[a]	94.83(7)	N1–Ru–X1B[b]	100.62(7)
N2–Ru–X1A[a]	100.99(7)	N2–Ru–X1B[b]	95.78(7)	C3–Ru–X1A[a]	91.25(7)	C3–Ru–X1B[b]	172.83(7)
C13–Ru–X1A[a]	172.37(7)	C13–Ru–X1B[b]	90.65(7)	X1A[a]–Ru–X1B[b]	82.12(7)		
3b							
Ru–N1	215.4(2)	Ru–C3	205.5(2)	Ru–N2	215.0(2)	Ru–C14	205.2(2)
Ru–C23	228.5(2)	Ru–C24	229.8(2)	Ru–C27	227.4(2)	Ru–C28	228.9(2)
N1–C1	129.7(3)	C1–C2	142.2(3)	C2–C3	135.9(3)	N2–C12	129.8(2)
C12–C13	141.9(3)	C13–C14	136.2(3)				
N1–Ru–N2	157.26(6)	N1–Ru–C3	77.30(7)	N1–Ru–C14	87.25(7)	N2–Ru–C3	88.08(7)
N2–Ru–C14	77.35(7)	C3–Ru–C14	97.32(7)	N1–Ru–X1A[a]	95.62(7)	N1–Ru–X1B[b]	101.72(7)
N2–Ru–X1A[a]	101.71(7)	N2–Ru–X1B[b]	95.34(7)	C3–Ru–X1A[a]	89.48(7)	C3–Ru–X1B[b]	171.38(7)
C14–Ru–X1A[a]	172.95(7)	C14–Ru–X1B[b]	91.24(7)	X1A[a]–Ru–X1B[b]	82.03(7)		
4							
Ru–N1	215.4(4)	Ru–C1	206.2(5)	Ru–C2	215.4(5)	Ru–N2	202.1(4)
Ru–N3	208.5(4)	Ru–C33	200.6(5)	N1–C1	141.5(6)	C1–C2	139.9(6)
C2–C3	143.8(7)	C3–C18	141.5(6)	C18–C17	139.2(7)	C17–C16	140.8(7)
C16–N2	132.9(6)	N3–C31	130.4(6)	C31–C32	140.7(7)	C32–C33	137.2(7)
N1–Ru–N2	161.3(2)	N1–Ru–N3	107.2(2)	N1–Ru–C33	92.9(2)	N1–Ru–X1A[c]	53.16(9)
N2–Ru–N3	90.5(2)	N2–Ru–C33	96.9(2)	N2–Ru–X1A[c]	108.3(2)	N3–Ru–C33	78.1(2)
N3–Ru–X1A[c]	158.0(2)	C33–Ru–X1A[c]	109.8(2)				

[a] Centroid of C21–C28 (**3a**) or C23–C24 (**3b**).
[b] Centroid of C24–C25 (**3a**) or C27–C28 (**3b**).
[c] Centroid of C1–C2 (**4**).

adopt both potential chair conformations most probably due to steric strain in the molecule. Therefore for one of the cyclohexyl groups 3 CH_2 signals each are observed whereas the others with reduced flexibility show 5 different CH_2 signals.

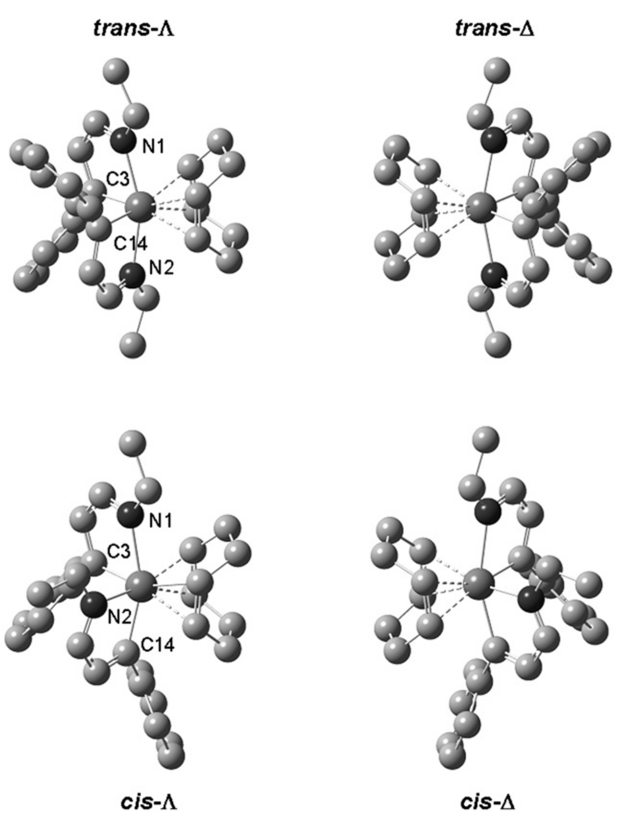

Fig. 3. Molecular structures of pairs of Λ- and Δ-enantiomers with nitrogen donor atoms either in *cis*- or *trans*-position calculated by DFT methods.

In additional experiments we wanted to know whether complex **1** is a suitable precatalyst for the synthesis of heterocyclic compounds from the respective cinnamaldehyde derived imines **2**. If this was true, coordination of the imine after C–H activation in terms of an enyl-imino ligand can be considered to be a suitable model for the coordination of the substrate at the mononuclear ruthenium catalyst species in early stages of the catalytic cycle. Up to know we used $Ru_3(CO)_{12}$ as precatalyst but we were nevertheless able to show that the catalytically active species is mononuclear [4h]. We therefore reacted **2a** with CO and C_2H_4 in an autoclave in the presence of catalytic amounts of **1**. As solvent we chose toluene and due to our most recent experiments concerning the use of ionic liquids we also performed the reaction in [C_4mim][BTA] (1-butyl-3-methylimidazolium-bis(trifluorsulfonyl)-imid, Scheme 2) [7]. For comparatibility reasons the experiments in the ionic liquid were also performed at variable temperatures with $Ru_3(CO)_{12}$ and with **1** as precatalyst. We have shown before that compounds **5** and **6** are most probably formed by an initial C–H activation in β-position with respect to the imine double bond in substrates of type **2** followed by ring closure and addition and insertion of the respective alkene [4f–k]. By the use of ^{13}C labeled carbon monoxide we were also able to demonstrate that C-2 of the pyrrole derivatives originates from carbon monoxide and that $^{13}CO_2$ is formed in the same stoichiometric ratio as pyrroles of type **6** [4j]. Products **5** and **6** are easily identified by their respective ^{1}H NMR spectra due to two doublets each representing hydrogen atoms attached to the heterocycle at characteristic chemical shifts. Corresponding NMR spectra from the crude reaction mixtures in all cases prove the quantitative consumption of the imine **2a** and the exclusive formation of mixtures of **5** and **6** (*cf.* Supplementary material). If reactions in [C_4mim][BTA] are performed at variable temperatures in the presence of either $Ru_3(CO)_{12}$ or **1** it can be seen that the mononuclear catalyst precursor works at slightly lower temperatures (Fig. 5). Most probably this corresponds to the inevitable cleavage of the cluster core in $Ru_3(CO)_{12}$.

Table 2
Selected bond lengths [pm] and angles [deg] of the calculated structures *trans*- and *cis*-**3b**.

trans-**3b**							
Ru–N1	219.3	Ru–N2	219.3	Ru–C3	206.3	Ru–C14	206.3
Ru–C_{COD}	235.0						
N1–Ru–N2	159.2	N1–Ru–C3	77.4	N1–Ru–C14	88.7	N2–Ru–C3	88.7
N2–Ru–C14	77.4	C3–Ru–C14	98.2				
cis-**3b**							
Ru–N1	230.2	Ru–N2	215.4	Ru–C3	208.3	Ru–C14	213.0
Ru–C_{COD}	228.9						
N1–Ru–N2	86.4	N1–Ru–C3	76.8	N1–Ru–C14	159.1	N2–Ru–C3	94.0
N2–Ru–C14	77.7	C3–Ru–C14	90.8				

As it has been demonstrated by some of us before use of toluene as solvent promotes the formation of **5** irrespective of the used precatalyst (ratio **5**:**6** in toluene: 90:10 ($Ru_3(CO)_{12}$), 95:5 (**1**); in [C_4mim][BTA]: 70:30 ($Ru_3(CO)_{12}$), 40:60 (**1**)) [4l,7]. Nevertheless, use of the mononuclear precursor **1** seems to further enhance the yield of **5** in toluene but the yield of **6** in the ionic liquid.

It can therefore be concluded that the coordination mode of deprotonated imine ligands in **3a**, **3b** and **4** can be considered to be a plausible model for the coordination of the respective substrates to ruthenium during catalytical reactions. Besides, the formation of **4** working *via* the reductive coupling of two imines can be considered to be highly related to the reaction of the same substrates in the presence of a large excess of CO and C_2H_4.

3. Experimental

All procedures were carried out under an argon atmosphere in anhydrous, freshly distilled solvents. NMR spectra were recorded on a Bruker DRX 400 spectrometer (^{1}H: 400,13 MHz, ^{13}C: 100.62 MHz, solvent as internal standard). Mass spectra were recorded on a Finnigan MAT SSQ 710 instrument. Elemental analyses were carried out at the laboratory of the Institute of Organic Chemistry and Macromolecular Chemistry of the Friedrich-Schiller-University Jena.

3.1. X-ray structure determinations

Intensity data were collected on a Nonius Kappa CCD diffractometer using graphite-monochromated Mo Kα radiation. Data

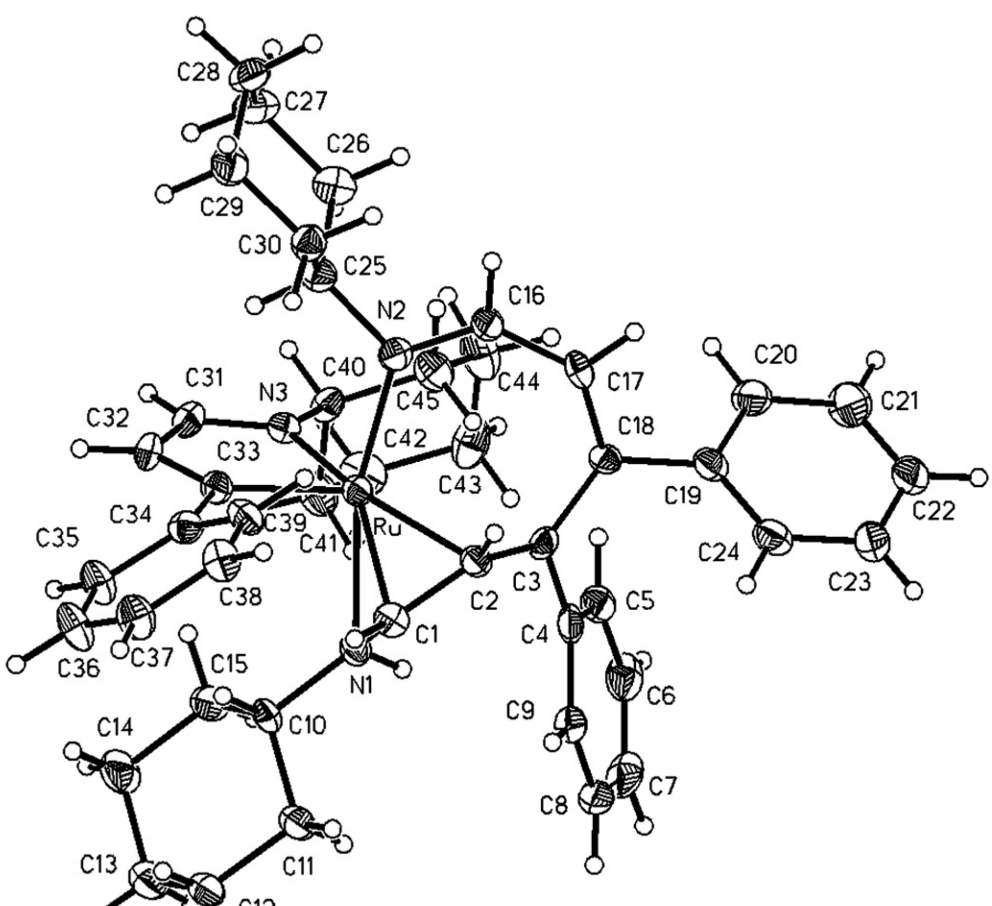

Fig. 4. Molecular structure of **4**. Thermal ellipsoids are depicted on the 40% probability level.

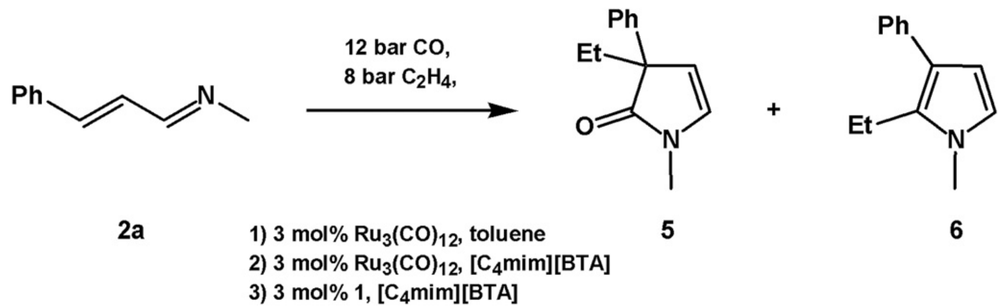

Scheme 2. Catalytic synthesis of 1,3-dihydropyrrolone **5** and pyrrole **6**.

were corrected for Lorentz polarization and not for absorption effects [8,9]. Crystallographic data as well as structure solution and refinement details are summarized in Table 3. The structures were solved by direct methods (SHELXS) and refined by full-matrix least squares techniques against F_o^2 (SHELXL-97) [10,11]. The hydrogen atoms were included at calculated positions with fixed thermal parameters. All non-hydrogen atoms were refined anisotropically. XP (SIEMENS Analytical X-ray Instruments, Inc.) was used for structure representations.

4. Synthesis of 3a, 3b and 4

300 mg **1** (0.94 mmol) are suspended in 15 n-pentane together with a two-fold excess of the corresponding imine (**2a**: 273 mg, **2b**: 300 mg, **2c**: 400 mg) and the mixture is then refluxed for 4 h. After cooling down to room temperature in the reaction of **2a** a small amount of a non-identified decomposition product has precipitated which is filtered off. The remaining solution is evaporated *in vacuo* and the resulting reddish brown oily residue is recrystallized from mixtures of pentane and dichloromethane at −40 °C leading to the isolation of **3a** (317 mg, 68%), **3b** (146 mg, 42%) and **4** (256 mg, 37%, all yields based on Ru) from the respective reaction mixtures.

4.1. MS and NMR data for ***3a***

MS (DEI) [m/z (%)]: 498 (MH^+, 2), 390 (MH^+−COD, 81), 245 (MH^+−COD−$C_{10}H_{10}N$, 5), 144 ($C_{10}H_{10}N^+$, 100), 129 ($C_9H_7N^+$, 8), 115 ($C_9H_7^+$, 17), 102 ($C_8H_6^+$, 10), 91 ($C_7H_7^+$, 11), 79 ($C_6H_7^+$, 35), 67 ($C_5H_7^+$, 39), 53 ($C_4H_5^+$, 31), 39 ($C_3H_3^+$, 35), 27 ($C_2H_3^+$, 23); ^{1}H NMR (400 MHz, $CDCl_3$, 298 K) [ppm]: 1.90–1.99 (m, 2H, CH_2), 2.10–2.18 (m, 2H, CH_2), 2.24–2.33 (m, 2H, CH_2), 2.53–2.58 (m, 2H, CH_2), 2.85 (s, 6H, CH_3), 2.91–2.95 (m, 1H, =CH), 4.19–4.25 (m, 1H, =CH), 6.26 (d, J_{HH} = 4.0 Hz, 2H, C_βH), 6.62 (m, 4H, C_{ar}H), 7.08–7.17 (m, 6H, C_{ar}H), 7.79 (d, J_{HH} = 4.0 Hz, 2H, C_αH); ^{13}C NMR (100.62 MHz, $CDCl_3$, 298 K) [ppm]: 28.0 (CH_2), 29.4 (CH_2), 48.6 (CH_3), 89.1 (=CH), 104.0 (=CH), 124.0 (C_{ar}H), 124.8 (C_{ar}H), 126.6 (C_αH), 129.9 (C_{ar}H), 154,4 (C_{ar}), 169.0 (C_{im}H), 231.6 (C_β); Anal. Calc. for $C_{28}H_{32}N_2Ru$: C, 67.61; H, 6.44; N, 5.63. Found: C, 67.41; H, 6.87; N, 5.39%.

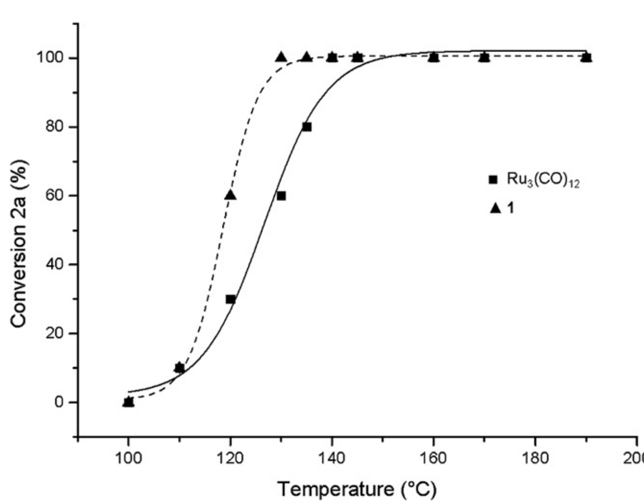

Fig. 5. Rate of conversion of **2a** depending on the choice of precatalyst ($Ru_3(CO)_{12}$ or **1**).

4.2. MS and NMR data for ***3b***

MS (DEI) [m/z (%)]: 417 (M^+−COD, 1), 260 (MH^+−COD−$C_{11}H_{12}N$, 6), 158 ($C_{11}H_{12}N^+$, 100), 143 ($C_{10}H_9N^+$, 11), 129 ($C_9H_7N^+$, 15), 115 ($C_9H_7^+$, 27), 91 ($C_7H_7^+$, 32), 79 ($C_6H_7^+$, 20), 67 ($C_5H_7^+$, 27), 56 ($C_4H_8^+$, 35), 41 ($C_3H_5^+$, 33), 27 ($C_2H_3^+$, 11); ^{1}H NMR (400 MHz, $CDCl_3$, 298 K) [ppm]: 1.27 (t, J_{HH} = 7.0 Hz, 6H, CH_3), 1.70–1.95 (m, 4H, CH_2), 1.98–2.21 (m, 2H, CH_2), 2.68–3.15 (m, 3H, CH_2, =CH), 3.56 (q, J_{HH} = 7.0 Hz, 4H, CH_2), 3.95–4.02 (m, 1H, =CH), 6.93–6.96 (m, 6H, C_βH, C_{ar}H), 7.30–7.56 (m, 6H, C_{ar}H), 8.07 (d, J_{HH} = 6.0 Hz, 2H, C_αH); ^{13}C NMR (100.62 MHz, $CDCl_3$, 298 K) [ppm]: 16.5 (CH_3), 24.2 (CH_2), 24.8 (CH_2), 56.1 (CH_2), 70.7 (=CH), 88.2 (=CH), 127.5 (C_{ar}H), 128.9 (C_{ar}H), 129.0 (C_αH), 129.1 (C_{ar}H), 136,3 (C_{ar}), 161.9 (C_{im}H), 236.3 (C_β); Anal. Calc. for $C_{30}H_{36}N_2Ru$: C, 68.57; H, 6.86; N, 5.33. Found: C, 67.92; H, 7.01; N, 5.48%.

Table 3
Crystal data and refinement details for the X-ray structure determinations of **3a**, **3b** and **4**.

Compound	3a	3b	4
Formula	$C_{28}H_{32}N_2Ru$	$C_{30}H_{36}N_2Ru$	$C_{45}H_{55}N_3Ru$
fw (g mol^{-1})	497.63	525.68	738.99
T/°C	−90(2)	−90(2)	−90(2)
Crystal system	Triclinic	Monoclinic	Monoclinic
Space group	$P\overline{1}$	$P2_1/c$	$P2_1/n$
a/Å	8.6212(3)	11.4875(2)	14.7977(11)
b/Å	11.6932(3)	16.2104(4)	15.1567(7)
c/Å	12.8748(3)	14.2967(4)	18.3657(13)
α/°	68.916(2)	90	90
β/°	80.298(2)	110.192(2)	113.505(3)
χ/°	71.849(2)	90	90
V/Å^3	1148.42(6)	2498.67(10)	3777.4(4)
Z	2	4	4
ρ (g cm^{-3})	1.439	1.397	1.299
μ (cm^{-1})	7.00	6.48	4.5
measured data	7706	16 727	26 485
data with $I > 2\sigma(I)$	4774	4783	4328
unique data/R_{int}	5070/0.0160	5665/0.0298	8606/0.1949
wR_2 (all data, on F^2)[a]	0.0653	0.0656	0.1294
R_1 ($I > 2\sigma(I)$)[a]	0.0245	0.0259	0.0700
s[b]	1.004	1.005	0.988
Res. dens./e Å^{-3}	0.437/−0.608	0.314/−0.464	0.470/−0.487
CCDC No.	763991	763992	763993

[a] Definition of the R indices: $R_1 = (\Sigma|F_o| - |F_c|)/\Sigma|F_o|$; $wR_2 = \{\Sigma[w(F_o^2 - F_c^2)^2]/\Sigma[w(F_o^2)^2]\}^{1/2}$ with $w^{-1} = \sigma^2(F_o^2) + (aP)^2 + bP$; $P = [2F_c^2 + \max(F_o^2)]/3$.
[b] $s = \{\Sigma[w(F_o^2 - F_c^2)^2]/(N_o - N_p)\}^{1/2}$.

4.3. MS and NMR data for **4**

MS (FAB) [m/z (%)]: 739 (MH^+, 1), 524 ($M^+-C_{15}H_{20}N$, 1), 424 ($M^+-C_{15}H_{20}N-C_6H_{14}N$, 1), 317 ($C_{15}H_{22}NRu^+$ 15), 213 ($C_{15}H_{19}N^+$, 100), 184 ($C_{13}H_{14}N^+$, 23), 170 ($C_{12}H_{12}N^+$, 44), 156 ($C_{11}H_{10}N^+$, 48), 131 ($C_9H_9N^+$, 46), 115 ($C_9H_7^+$, 69), 91 ($C_7H_7^+$, 48), 77 ($C_6H_5^+$, 23), 65 ($C_5H_5^+$, 27), 55 ($C_4H_7^+$, 37), 41 ($C_3H_5^+$, 43), 27 ($C_2H_3^+$, 15); ^{1}H NMR (400 MHz, CD_2Cl_2, 298 K) [ppm]: 0.81–1.85 (m, 31H, CH, CH_2), 3.18–3.38 (m, 2H, CH), 4.57 (d, 1H, J_{HH} = 4.9 Hz, =CH), 5.59 (d, 1H, J_{HH} = 8.0 Hz, =CH), 6.62–6.67 (m, 3H, C_{ar}H), 6.82 (pseudo-t, J_{HH} = 7.1 Hz), 7.00–7.62 (m, 16H, C_{ar}H, NH), 8.13 (d, 1H, J_{HH} = 8.0 Hz, =CH), 8.21 (s, 1H, =CH), 9.70 (d, 1H, J_{HH} = 8.0 Hz, =CH); ^{13}C NMR (100.62 MHz, CD_2Cl_2, 298 K) [ppm]: 24.9 (CH_2), 25.5 (CH_2), 25.6 (CH_2), 25.7 (CH_2), 26.0 (CH_2), 26.2 (CH_2), 26.5 (CH_2), 33.0 (CH_2), 34.2 (CH_2), 35.7 (CH_2), 35.9 (CH_2), 36.0 (CH_2), 37.1 (CH_2), 60.6 (CH), 67.2 (CH), 69.8 (CH), 73.2 (CH), 82.8 (=C), 86.3 (=CH), 104.5 (=CH), 123.4 (=C), 125.3 (=CH), 125.7 (C_{ar}H), 126.8 (C_{ar}H), 127.1 (C_{ar}H), 127.8 (C_{ar}H), 128.8 (C_{ar}H), 129.4 (C_{ar}H), 129.8 (C_{ar}H), 131.5 (C_{ar}H), 132.4 (=CH), 135.0 (C_{ar}H), 141.5 (C_{ar}), 143.7 (C_{ar}), 146.7 (C_{ar}), 151.0 (=CH), 164.2 (=CH), 193.8 (=C); Anal. Calc. for $C_{45}H_{55}N_3Ru$: C, 73.17; H, 7.45; N, 5.69. Found: C, 72.34; H, 7.69; N, 5.36%.

5. Synthesis of 5 and 6

In a typical reaction a 50 cm^3 autoclave was charged with 145 mg (1 mmol) methyl(3-phenylallylidene)amine, **2a**, 19 mg (0.03 mmol) $Ru_3(CO)_{12}$ or 10 mg (0.03 mol) [(COD)Ru(C_4H_7)$_2$], **1**, and 5 cm^3 toluene or [C_4mim][BTA]. The autoclave then was pressurized with 12 bar carbon monoxide and 8 bar ethylene and heated. If **1** was present as the precatalyst the reaction temperature was varied between 100 and 190 °C. The reaction mixture was vigorously stirred for 10 h. After the reaction mixture was cooled to room temperature it was transferred to a Schlenk tube. In case of toluene as the solvent the reaction mixture was evaporated *in vacuo* and the oily residue was used to determine the yield of **5** and **6** by ^{1}H NMR spectroscopy (for a complete characterisation see Ref. [4j] from our group). If the ionic liquid was used as reaction medium 10 mL of anhydrous diethylether was added. Complete extraction of the reaction products to the organic phase was achieved by stirring the biphasic mixture at room temperature overnight. After separation of the organic phase from the ionic liquid phase diethylether was removed *in vacuo* and the remaining oily residue was used to determine yields of the products **5** and **6** by ^{1}H NMR spectroscopy. If resonances corresponding to the respective ionic liquid were observed the residue was redissolved in diethylether and the solution filtered on silica. After evaporation of the solvent ^{1}H NMR spectroscopy was used to check whether the ionic liquid has been completely removed from the product compounds.

5.1. NMR data for **5**

^{1}H NMR (200 MHz, $CDCl_3$, 298 K) [ppm]: 0.79 (t, 3H, J_{HH} = 7.1 Hz, CH_3), 1.99 (q, 2H, J_{HH} = 7.1 Hz, CH_2), 3.01 (s, 3H, N–CH_3), 5.63 (d, 1H, J_{HH} = 4.3 Hz, =CH), 6.47 (d, 1H, J_{HH} = 4.3 Hz, =CH), 6.95–7.56 (m, 5H, Ph).

5.2. NMR data for **6**

^{1}H NMR (200 MHz, $CDCl_3$, 298 K) [ppm]: 1.22 (t, 3H, J_{HH} = 7.5 Hz, CH_3), 2.71 (q, 2H, J_{HH} = 7.5 Hz, CH_2), 3.60 (s, 3H, N–CH_3), 6.21 (d, 1H, J_{HH} = 2.8 Hz, =CH), 6.55 (d, 1H, J_{HH} = 2.8 Hz, =CH), 6.95–7.56 (m, 5H, Ph).

Appendix A. Supplementary material

A listing of data collection and refinement procedures as well as positional coordinates of all atoms (CIF files). This material is available free of charge via the Internet at http:/pubs.acs.org. In addition, the data deposited at the Cambridge Crystallographic Data Centre under CCDC-763991 for **3a**, -763992 for **3b**, and -763993 for **4** contain the supplementary crystallographic data for this paper. These data can be obtained free of charge from The Cambridge Crystallographic Data Centre via www.ccdc.cam.ac.uk/conts/retrieving.html.^{1}H NMR spectra of reaction mixtures from catalytic reactions using **1** as precatalyst in [C_4mim][BTA] (Fig. S1) or in toluene (Fig. S2) and headspace GC-MS spectra from a sealed Schlenk tube in which **1** and **2a** are reacted (Fig. S3) are also available as supplementary material.

Supplementary data associated with this article can be found, in the online version, at doi:10.1016/j.jorganchem.2010.05.020.

References

[1] C.J. Elsevier, W.P. Mul, K. Vrieze, Inorg. Chim. Acta 198–200 (1992) 689.
[2] (a) L.H. Polm, W.P. Mul, C.J. Elsevier, K. Vrieze, M.J.N. Christophersen, C. H. Stam, Organometallics 7 (1988) 423;
(b) W.P. Mul, C.J. Elsevier, K. Vrieze, W.J.J. Smeets, A.L. Spek, Rec. Trav. Chim. Pays-Bas 107 (1988) 297;
(c) O.C.P. Beers, C.J. Elsevier, W.P. Mul, K. Vrieze, L.P. Haming, C.H. Stam, Inorg. Chim. Acta 171 (1990) 129;
(d) W.P. Mul, C.J. Elsevier, M. van Leijen, K. Vrieze, A.L. Spek, Organometallics 10 (1991) 533;
(e) W.P. Mul, C.J. Elsevier, W.J.J. Smeets, A.L. Spek, Inorg. Chem. 30 (1991) 4152;
(f) A.L. Spek, A.J.M. Duisenberg, W.P. Mul, O.C.P. Beers, C.J. Elsevier, Acta Cryst. C 47 (1991) 297;
(g) O.C.P. Beers, C.J. Elsevier, H. Kooijman, W.J.J. Smeets, A.L. Spek, Organometallics 12 (1993) 3187;
(h) O.C.P. Beers, M.M. Bouman, A.E. Komen, K. Vrieze, C.J. Elsevier, E. Horn, A. L. Spek, Organometallics 12 (1993) 315;
(i) O.C.P. Beers, C.J. Elsevier, W.J.J. Smeets, A.L. Spek, Organometallics 12 (1993) 3199;
(j) W. Imhof, J. Chem. Soc., Dalton Trans (1996) 1429.
[3] O.C.P. Beers, M.M. Bouman, C.J. Elsevier, W.J.J. Smeets, A.L. Spek, Inorg. Chem. 32 (1993) 3015.
[4] (a) G. Dyker, Angew. Chem. Int. Ed. Engl. 38 (1999) 1698;
(b) Y. Guari, S. Sabo-Etienne, B. Chaudret, Eur. J. Inorg. Chem. (1999) 1047;
(c) F. Kakiuchi, S. Murai, Top. Organomet. Chem. 3 (1999) 47;
(d) V. Ritleng, C. Sirlin, M. Pfeffer, Chem. Rev. 102 (2002) 1731;
(e) N. Chatani, Chem. Rec. 8 (2008) 201;
(f) D. Berger, W. Imhof, J. Chem. Soc., Chem. Commun. (1999) 1457;
(g) D. Berger, W. Imhof, Tetrahedron 56 (2000) 2015;
(h) D. Berger, A. Göbel, W. Imhof, J. Mol. Catal. A: Chem. 165 (2001) 37;
(i) W. Imhof, D. Berger, M. Kötteritzsch, M. Rost, B. Schönecker, Adv. Synth. Catal. 343 (2001) 795;
(j) D. Dönnecke, W. Imhof, Tetrahedron 59 (2003) 8499.(k) W. Imhof, A. Göbel, J. Organomet. Chem. 690 (2005) 1092;
(l) G. Gillies, D. Dönnecke, W. Imhof, Monatsh. Chem. 138 (2007) 683.
[5] M.J. Frisch, G.W. Trucks, H.B. Schlegel, G.E. Scuseria, M.A. Robb, R. J. Cheeseman, J.A. Montgomery Jr., T. Vreven, K.N. Kudin, J.C. Burant, J. M. Millam, S.S. Iyengar, J. Tomasi, V. Barone, B. Mennucci, M. Cossi, G. Scalmani, N. Rega, G.A. Petersson, H. Nakatsuji, M. Hada, M. Ehara, K. Toyota, R. Fukuda, J. Hasegawa, M. Ishida, T. Nakajima, Y. Honda, O. Kitao, H. Nakai, M. Klene, X. Li, J.E. Knox, H.P. Hratchian, J.B. Cross, V. Bakken, C. Adamo, J. Jaramillo, R. Gomperts, R.E. Stratmann, O. Yazyev, A.J. Austin, R. Cammi, C. Pomelli, J.W. Ochterski, P.Y. Ayala, K. Morokuma, G.A. Voth, P. Salvador, J.J. Dannenberg, V.G. Zakrzewski, S. Dapprich, D.A. Daniels, M. C. Strain, O. Farkas, D.K. Malick, A.D. Rabuck, K. Raghavachari, J.B. Foresman, J. V. Ortiz, Q. Cui, A.G. Baboul, S. Clifford, J. Cioslowski, B.B. Stefanov, G. Liu, A. Liashenko, P. Piskorz, I. Komaromi, R.L. Martin, D.J. Fox, T. Keith, M.A. Al-Laham, C.Y. Peng, A. Nanayakkara, M. Challacombe, P.M.W. Gill, B. Johnson, W. Chen, M.W. Wong, C. Gonzalez, J.A. Pople, Gaussian 03, Revision D.01. Gaussian, Inc., Wallingford CT, 2004.
[6] W. Imhof, Organometallics 18 (1999) 4845.
[7] T. Biletzki, A. Stark, W. Imhof, Monatsh. Chem. 141 (2010) 413.
[8] COLLECT, Data Collection Software. Nonius B.V., Netherlands, 1998.
[9] Z. Otwinowski, W. Minor, Processing of X-ray diffraction data collected in oscillation mode. in: C.W. Carter, R.M. Sweet (Eds.), Methods in Enzymology, Macromolecular Crystallography, Part A, vol. 276. Academic Press, 1997, pp. 307–326.
[10] G.M. Sheldrick, Acta Crystallogr. A 46 (1990) 467–473.
[11] G.M. Sheldrick, SHELXL-97 (Release 97-2). University of Göttingen, Germany, 1997.